The Grimsel Migration Experiment: field injection–withdrawal experiments in fractured rock with sorbing tracers

E. Hoehn [a,*,1], J. Eikenberg [a], T. Fierz [b], W. Drost [c], E. Reichlmayr [c]

[a] *Paul Scherrer Institute, CH-5232 Villigen PSI, Switzerland*
[b] *Solexperts, Research and Consulting Office for Applied Rock and Soil Mechanics and Hydraulics, CH-8603 Schwerzenbach, Switzerland*
[c] *GSF-Institut für Hydrologie, D-85764 Neuherberg, Germany*

Abstract

In the framework of the Migration Experiment at the Grimsel Test Site, Switzerland, breakthrough experiments with a conservative tracer, uranine, and sorbing cationic γ-emitting radionuclides ($^{22,24}Na^+$, $^{85}Sr^{2+}$, $^{86}Rb^+$, and $^{137}Cs^+$) were carried out to test models of radionuclide migration in the field. An array of bore holes drilled from an experimental drift penetrated a transmissive, water-saturated shear zone in a granodiorite. The shear zone consists of a set of fractures filled with a fine-grained porous fault gouge. A two bore hole injection-withdrawal ('dipole') flow field was superimposed on the natural hydraulic gradient and two different linear flow distances, 1.7 and 4.9 m, were studied in detail. The concentrations of the radionuclides were, in general, much smaller than the natural background levels of the corresponding stable isotopes of Na, Sr, Rb, and Cs, in the groundwater of the shear zone. In-line tracer detection techniques included down-hole point fluorescence measurement and NaI scintillation counting of γ-emitters in the withdrawal flow line. Pulse-stimulus tracer injections resulted in monomodal breakthrough curves and recovery curves. The reduction of the maximum (peak) radionuclide activity (relative to the injected activity), peak retardation, and retardation of the time of 50% recovery were compared to those of uranine. A selectivity sequence of relative affinity of the studied cations for an exchange site was found to be Na ($<$ Ca) $<$ Sr $<$ Rb $<$ Cs. In the shorter flow field, the radionuclides exhibited little peak-height reduction relative to uranine and little or

---

* Corresponding author. Fax: +41-1-823-5028; e-mail: hoehn@eawag.ch
[1] Present address: EAWAG, Swiss Federal Institute for Environmental Science and Technology, CH-8600 Dübendorf, Switzerland.

no retardation. In the longer flow field, Sr and Cs showed a considerable peak-height reduction and a significant retardation relative to uranine and Na. Increasing the flow distance affected the retardation of the radionuclides. The results were compared with both pre- and post-experiment model simulations and earlier model predictions.

1. Introduction

In the multi-barrier system of a radioactive waste repository, the geosphere represents an important component (Hadermann et al., 1988; NAGRA, 1994) and this barrier function can be evaluated in field studies. Field experiments with reactive radionuclide solutions and non-sorbing (chemically inert = conservative) tracers are valuable to confirm the physical and chemical data obtained from laboratory experiments (batch and dynamic), and to test model predictions of radionuclide migration in subsurface situations. The Swiss National Cooperative for the Disposal of Radioactive Wastes (NAGRA) has conducted a variety of experiments at the Grimsel Test Site (GTS) in central Switzerland. The site is located near the headwaters of the river Aare, about 450 m below surface at an elevation of about 1730 m a.s.l. Among the experiments, a joint NAGRA/PNC (Japanese Power Reactor and Nuclear Fuel Development) funded study of the migration of radionuclides (Migration Experiment) at the GTS aimed at a better understanding of solute transport in a fractured rock. The Migration Experiment is embedded in an overall Migration Program which includes among other work the excavation of part of the studied fracture system. The Migration Experiment benefited from the experience gained in prior studies of field tracer experiments in underground facilities of fractured rock (e.g., Finnsjön, Sweden: Neretnieks et al., 1982; Studsvik, Sweden: Klockars et al., 1983). Overviews of the work are given in McKinley et al. (1988), Frick et al. (1992) and Frick (1994).

The major aim of the interdisciplinary Migration Experiment is to extrapolate laboratory sorption data to field conditions and identify the relevant transport processes in the field, and to demonstrate the applicability of a methodology for the testing of radionuclide transport models (McKinley et al., 1988; Frick, 1994). Up to 1994, field work at the site consisted of 90 individual tracer experiments with non-sorbing tracers and weakly- to strongly-sorbing γ-ray emitting radionuclides of alkaline and alkaline-earth metals, $^{22}Na^+$, $^{24}Na^+$, $^{85}Sr^{2+}$, $^{86}Rb^+$, and $^{137}Cs^+$. In this group, $^{85}Sr^{2+}$ and $^{137}Cs^+$ are relevant to safety assessments of radioactive waste repositories. This paper presents the results of a subset of these experiments, carried out at two different distances in a transmissive shear zone in crystalline rock (Grimsel granodiorite). The influence of experimental conditions and effects of a variable flow distance on field-scale radionuclide retardation are also discussed.

The mineralogy and structural geology has been described in Meyer et al. (1989) and Bossart and Mazurek (1991). The genetic development of the shear zone is as follows: during post-metamorphic Alpine uplift, processes of brittle deformation in the granodior-ite reactivated ductile shear zones from the Hercynian orogenesis. These processes

resulted in a small number of interconnected fractures, partly filled with highly porous (10–30%) micaceous fault gouge producing zones of high transmissivity (Bossart and Mazurek, 1991). The shear zone chosen for the tracer experiments was explored with eight bore holes (Fig. 1) and was found to be an almost planar asymmetrical array of small fractures of a total width of 0.001–0.1 m. In this zone, the groundwater discharges into the GTS drift from five distinct channels, at a total flow rate of about 0.5 l min^{-1}. The intervals of the bore holes which intersect the shear zone are isolated with packers, to avoid the distortion of the flow field, and for hydraulic testing and sampling of groundwater (Hoehn et al., 1990). The drilling resulted in a local drainage of groundwaters, but steady discharge rates and hydraulic pressures at saturated flow conditions were re-established in the flow field before the start of the experiments. They remained constant over the time scale of typical experiments.

The mineralogy of the fault gouge in the shear zone and the surrounding granodiorite is similar (quartz, plagioclase-albite, K-felspar, biotite, muscovite, and chlorite; e.g., Meyer et al., 1989; Frick et al., 1992). Eikenberg et al. (1991) estimated an in situ cation exchange capacity of the material in the shear-zone from a hydrogeochemical equilibrium experiment to be in the order of 1–5 meq g^{-1}. Ca^{2+} and Na^+ contribute to > 99% to the positive charge of the groundwater, and alkalinity and F^- to about 70% of the negative charge (groundwater composition given in Table 1). Concentrations of
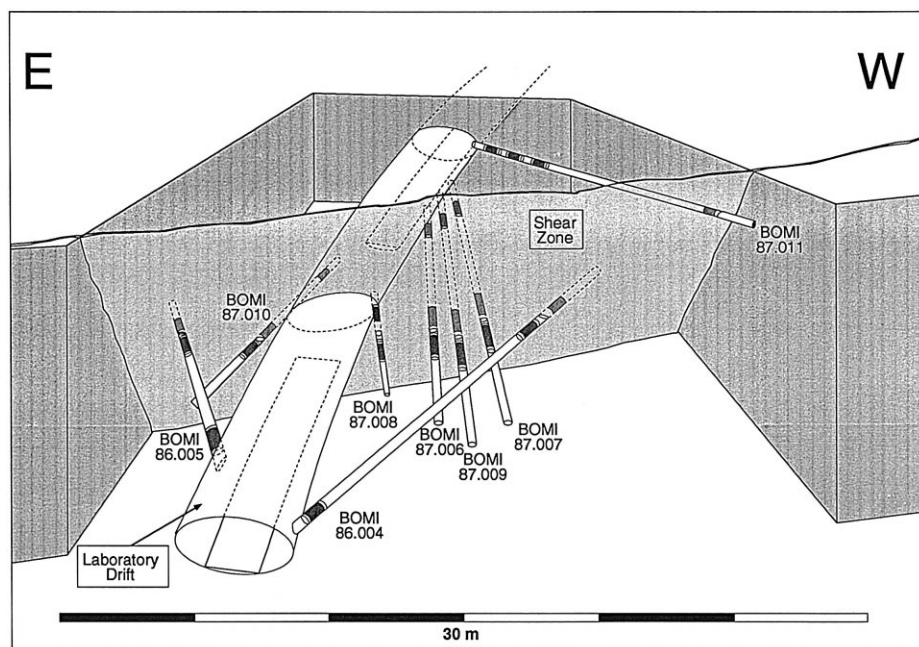

Fig. 1. Three-dimensional perspective view of Migration Site, showing eight exploration bore holes drilled from laboratory drift into migration shear zone, bore holes inclined downwardly (except BOMI 87.011), to ensure air-tight conditions: (BOMI 86.004–86.005, and BOMI 87.006–87.010, length 6–24 m; Frick et al., 1992).

Table 1
Chemical composition of groundwater discharging from migration shear zone into GTS drift (compiled from Bajo et al. (1989), Aksoyoglu et al. (1990), Frick et al. (1992), and Eikenberg et al. (1994))

	pH		9.6 ± 0.2
	Ionic strength	[M]	1.2×10^{-3}
	Temperature	[°C]	12 ± 1
	Electric conductivity	[$\mu S\ cm^{-1}$]	103 ± 5
Cations	Na^+	[M]	6.9×10^{-4}
	K^+	[M]	$3.8–5.0 \times 10^{-6}$
	Mg^{2+}	[M]	$5.4–6.2 \times 10^{-7}$
	Ca^{2+}	[M]	$1.3–1.4 \times 10^{-4}$
	Sr^{2+}	[M]	$1.8–2.0 \times 10^{-6}$
	Fe(total)	[M]	3×10^{-9}
	Mn(total)	[M]	5×10^{-9}
	Rb^+	[M]	2.5×10^{-8}
	Cs^+	[M]	5×10^{-9}
	NH_4^+	[M]	5×10^{-10}
	Cu(total)	[M]	6×10^{-10}
	U(total)	[M]	6×10^{-10}
Anions	SO_4^{2-}	[M]	$5.7–6.1 \times 10^{-5}$
	F^-	[M]	$3.3–3.6 \times 10^{-4}$
	Cl^-	[M]	$1.5–1.6 \times 10^{-4}$
	Br^-	[M]	3.8×10^{-7}
	I^-	[M]	1.0×10^{-9}
	Alkalinity	[eq l^{-1}]	$4.2–4.5 \times 10^{-4}$
Other species	Si	[M]	2.5×10^{-4}
	CO_2	[M]	$< 10^{-7}$
	O_2	[M]	$< 3 \times 10^{-8}$
	N_2	[M]	$7–8 \times 10^{-4}$

dissolved O_2 and CO_2 were always below detection limit. The high pH of 9.6 probably reflects various proton- and CO_2-consuming weathering reactions with silicates. The buffering of pH is caused mainly by the two systems $H_4SiO_4/H_3SiO_4^-$ (including solid amorphous SiO_2) and CO_3^{2-}/HCO_3^-. Electrode Eh values were considered meaningless due to the low concentration of electrode relevant species (see Frick et al., 1992, and Table 1). Monitoring over a period of about 1 year revealed spatial and temporal variations of groundwater temperature and concentrations of the main and trace components of less than $\pm 20\%$ (Eikenberg et al., 1991).

2. Experimental

2.1. Flow field

For the tracer experiments, a steady two bore hole injection–withdrawal (dipole) groundwater flow field was superimposed on the natural flow field. The dipole arrange-
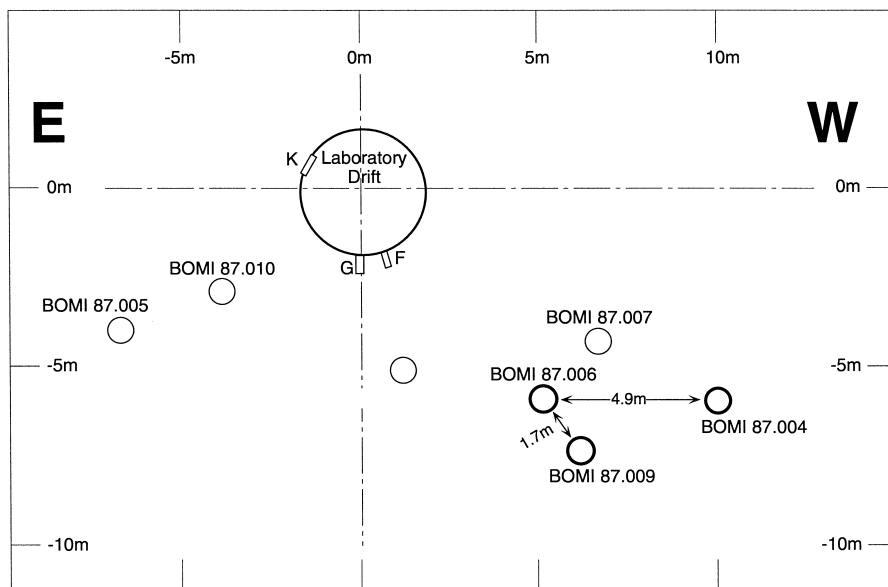
Fig. 2. Location of bore hole intersections with migration shear-zone, and linear flow distances between bore holes of shorter and longer flow field.

ment was preferred to an option with the GTS drift acting as an outlet for the withdrawal of tracers. It simplified the natural flow conditions, specifically avoiding: (i) uncontrolled withdrawal-flow rates to the drift and the presence of unsaturated zones and steep hydraulic gradients near the drift (drainage). Given a homogeneous aquifer with stagnant groundwater, the simplest dipole flow field exhibits symmetric flow and potential lines at identical flow rates (e.g., Nowakowski et al., 1985). In the GTS Migration Experi-

Table 2
Data on flow field (from Hoehn et al., 1990)

Transmissivity[a]	$2.2 \pm 0.7 \times 10^{-6}$ m^2 s^{-1} (average $\pm 1\sigma$)
Hydraulic pressure	
Injection intervals (BOMI 86.004 and 87.009)	1.2–1.3 bars (1 bar $\approx 10^5$ Pa)
Withdrawal interval (BOMI 86.006)	0.5–0.8 bars
Hydraulic conductivity of granodiorite matrix	About 10^{-11} m s^{-1}
Withdrawal-flow rate, Q_W:	
Flow distance: 4.9 m	150 ± 5 ml min^{-1}
Flow distance: 1.7 m	120 ± 5 ml min^{-1}
Injection-flow rate, Q_I:	
Flow distance: 4.9 m	10 ± 0.005 l min^{-1}
Flow distance: 1.7 m	8 ± 0.005 l min^{-1}
$\beta = Q_W / Q_I$	15 ± 1

[a] Passive single-hole and cross-hole hydraulic testing of six of the eight bore holes (two bore holes dry), constant pressure and constant discharge tests.
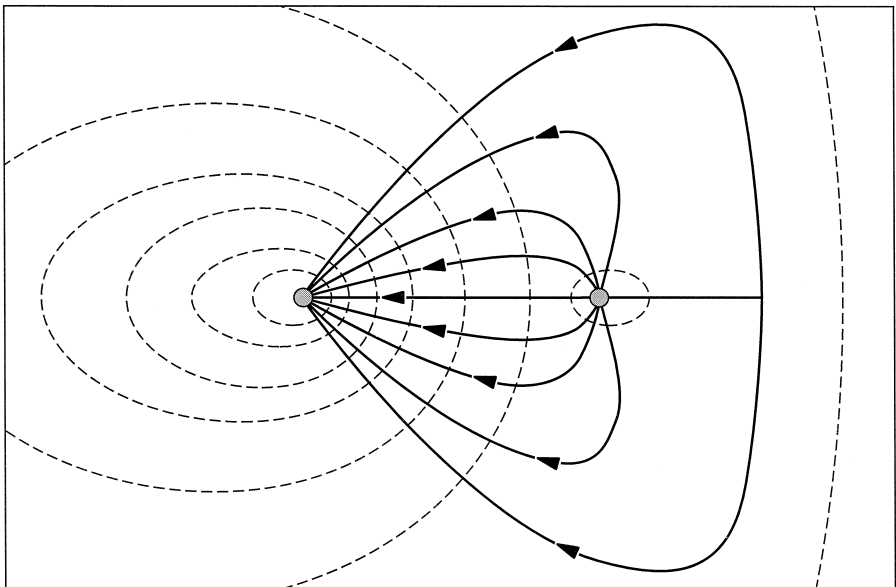
Fig. 3. Intersection of injection and withdrawal bore hole with shear-zone: full lines, ground-water flow lines; dashed lines, lines of equal groundwater potential. Domain bounded by flow lines contains tracered water.

ment, however, asymmetric dipole flow fields between the bore holes BOMI 86.004 and BOMI 87.006 (4.9 m flow distance, longer flow field), and BOMI 87.009 and BOMI 87.006 (1.7 m flow distance, shorter flow field) were used as they allowed optimization of the tracer recovery (see Fig. 2; data on flow field given in Table 2). The chosen combination of injection and withdrawal bore holes revealed flat hydraulic gradients between the packed-off sections, which minimized the influence of the radial flow field towards the drift (Hoehn et al., 1990). Flow lines which arrive at the withdrawal bore hole are partitioned into an inner domain containing the injected water, and an outer domain containing additional tracer-free groundwater. The additional water dilutes the injection water by a ratio (β in Table 2) of the withdrawal- to the injection-flow rate. Hadermann and Heer (1996) found that in flow fields with β sufficiently greater than one, virtually all flow lines starting at the injection bore hole end at the withdrawal bore hole (see Fig. 3). In the Migration Experiments with $\beta = 15$, less than 1% of the injected water was lost by flow to the GTS drift. Under these conditions, the flow field permeated by the injected water can be considered to be a bounded domain. In a perfectly bounded dipole-flow domain, an injection of conservative or reversibly-sorbing tracers results in a complete recovery after a sufficiently long period.

2.2. Tracers used

Conservative tracers were selected according to the following criteria (Frick et al., 1992), they should be: (i) non-reactive with the rock material in the shear zone and with

the experimental equipment; (ii) chemically stable and not affected by the natural groundwater composition; (iii) non-toxic, and environmentally safe; (iv) used in quantities which are easy to handle; (v) detectable in small quantities; (vi) analyzed on-line with standard techniques; (vii) below detection limits in the natural groundwater. The groundwater tracer uranine (Na-fluoresceine, e.g., Smart and Laidlaw, 1977) was used in the experiments discussed here because it had been shown to be stable and non-sorbing in the granitic environment of the Stripa test site in Sweden (Abelin et al., 1991). Its fluorescence intensity depends on pH due to a hydrolysis reaction (Behrens, 1983) and is high at values of pH of > 7. In addition, $^{82}Br^-$, ^4He, $^{123}I^-$, ^3H and ^3He were used as conservative tracers in other experiments not discussed here (see Eikenberg et al., 1992; Frick, 1994).

As sorbing tracers, Baeyens and Bradbury (1989) initially recommended the use of radioisotopes of the cations, Na^+ and Sr^{2+}, at concentrations at least 100 times below those of their stable isotopes in the groundwater (data on radionuclides used given in Table 3). From the results of laboratory experiments, these authors predicted that these cations would sorb reversibly on the fault-gouge material, with a linear isotherm and predominantly by an isotope-exchange mechanism. The magnitude of this sorption mechanism depends on the fractional occupancies of available sites on sheet-silica minerals. An experiment was first carried out in the longer flow field (see Fig. 2) with a cocktail of $^{22}Na^+$ and $^{85}Sr^{2+}$ (Run no. 50). Cocktails consisting of more than one reactive tracer were preferred to tests with only one reactive tracer, to ensure identical hydraulic conditions and to save time and costs. Later, a cocktail of $^{24}Na^+$ and $^{85}Sr^{2+}$ (Run no. 66) and, finally, a cocktail of $^{85}Sr^{2+}$ and $^{86}Rb^+$ (Run no. 75) were injected in the shorter flow field. $^{24}Na^+$ was preferred to $^{22}Na^+$ because its much shorter half life minimizes the risk of contaminating the site with radioactivity (see Table 3). The half-life of $^{24}Na^+$ was, however, not sufficiently long for experiments in the longer flow field. Cs^+ was then considered as a more strongly and possibly non-linearly sorbing tracer (Bradbury and Baeyens, 1992). $^{86}Rb^+$ was chosen first as a short-lived substitute of Cs isotopes as it was known to behave similarly. Later, two experiments with long-lived $^{137}Cs^+$ were carried out in the shorter flow field (Runs no. 80 and 86). In Experiment no. 80, the tracer was injected carrier-free, while in Experiment no. 86, carrier Cs was added to the radionuclide tracer. Finally, an experiment with $^{137}Cs^+$ was started in the longer flow field (Experiment no. 90).

Table 3
Data on radionuclide injection solutions

Radionuclide	Half-Life	Specific activity [GBq mg^{-1}]	Chemical compound[a]	Chemical species[b]
^{24}Na	15 h	0.37	Na_2CO_3	Na^+
^{22}Na	2.6 years	1.2	NaCl	Na^+
^{85}Sr	65 days	109	$SrCl_2$	Sr^{2+}
^{86}Rb	19 days	0.3	RbCl	Rb^+
^{137}Cs	30 days	0.63	CsCl	Cs^+

[a] In injection solution.
[b] In groundwater.

2.3. Equipment set-up

An identification of the various radionuclide transport processes requires high-quality experimental data (Heer and Hadermann, 1994). To obtain reliable tracer concentration data over several orders of magnitude and to guarantee undisturbed and steady hydraulic and stable hydrochemical conditions proved to be a demanding task in the field study described here. For example, experimental artefacts such as sorption on test equipment or instrumental dispersion due to dead volumes in lines and packed-off intervals had to be minimized. Early pilot tests (1988–1989) aimed primarily at characterizing the dipole flow field. Residence times of conservative tracers in the order of 1–10 h correspond to residence times of sorbing radionuclides between 10 h and more than a month, at retardation coefficients of 10 to 100. The flow rates of the pilot tests had to be adapted accordingly. The pilot tests showed a number of experimental problems to be solved, among them the following important set-up modifications and optimizations (Fig. 4; see also Frick, 1994; Eikenberg et al., 1994).

- Reduction of total dead volume of the instrumental set-up by one order of magnitude, from originally a few liters to a few 100 ml, to reduce the unknown instrumental dispersion.
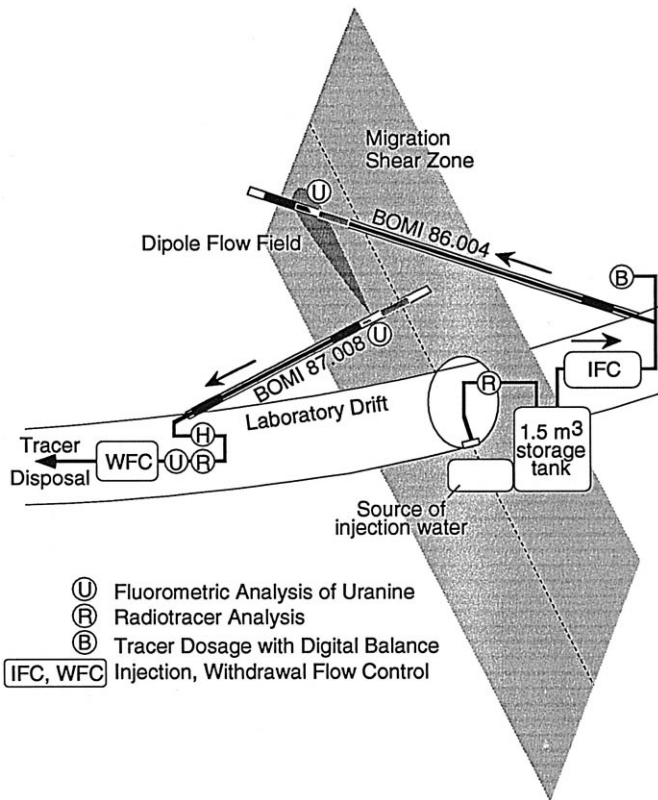
Fig. 4. Experimental set-up and location of tracer analytical equipment.

- Exclusive use of teflon-coated stainless steel, teflon and nylon, as materials for test equipment in direct contact with traced water, to avoid sorption of tracers on the equipment (for conclusions from material blank tests, see Eikenberg et al., 1994).

- Implementation of a HPLC pumping technique with very stable, precise and long-term constant pumping rates (SHIMADZU, LC-8), to provide and maintain a constant flow field during the experiments (requirement for transport modelling, see Heer and Hadermann, 1994).

- Use of groundwater from the site for dipole injection flow, including the installation of a stainless-steel reservoir tank without teflon coating, which was flushed with nitrogen gas (99.5% N_2, rest mainly O_2; Carbagas, Zurich, Switzerland), to keep the groundwater O_2- and CO_2-free (strong recommendation of Eikenberg et al., 1992).

- Monitoring of specific electrical conductivity, temperature, and pH of the injected and the withdrawn water with electrode probes (WTW 3000, Wissenschaftlich-Technische Werkstätten, Weilheim, Germany), and dissolved oxygen, with a sensitive flow cell (type 2713, Orbisphere, Geneva, Switzerland; detection limit: 0.01 ppb). On-line monitoring of these physico-chemical parameters was part of the stability control of the groundwater composition within the shear zone.

- Development of precise dosage devices for pulse and step input tracer mass determination, using a balance (PM 4600, Mettler Greifensee, Switzerland; detection limit: 1 mg), an additional HPLC pump for dosage, and a recirculation line for mixing and saturation of pump and lines with tracer solution, before injection into the dipole flow line (Eikenberg et al., 1994).

- Development and implementation of dual-quartz optical fluorometry in packer systems, to enable a precise and highly sensitive down-hole analysis of uranine: the signals downhole were modified with respect to those at the beginning of the injection flow line. Therefore, down-hole optical fluorometry was necessary to define the tracer concentration–time input function in the packed-off interval of the injection bore hole. It was furthermore helpful for monitoring tracer breakthrough in the packed-off interval of the withdrawal bore hole (for details, see Frick et al., 1992).

- Equipment tests (i.e., 'blank' tests) verified that the measured uranine input function is also valid for the simultaneously injected sorbing radionuclides, for which down-hole measurement was not feasible.

- Increase of the analytical range for on-line tracer detection devices to allow minimal injection of tracer mass or activity, e.g., using a high-resolution 17 bit data logger (Fluke Helios), development of data acquisition software, optimizing geometry of flow through devices for the on-line γ-spectrometry (ORTEC, 441; detection limit for counting intervals of 2 min: 50 Bq 1^{-1}, and 10 cm lead shielding to decrease the high γ-background scatter from natural terrestrial radiation). The conversion of measured signals into specific activity units (Bq 1^{-1}) was achieved by comparing laboratory results from check samples taken during the experiments with the corresponding on-line measured data (for details, see Eikenberg et al., 1994).

2.4. Radiation protection measures

Working with radioactive tracers requires radiation protection and a radiation-controlled zone was built in the GTS drift, which conformed to the Swiss radioprotection

regulations (HSK, 1993). Radiation protection measures specifically designed for the GTS Migration Experiment included the following elements (Frick, 1994).

- Access to the laboratory zone restricted to those involved in the Migration Experiment, and all work carried out in this zone monitored by a trained radioprotection officer (E. Reichlmayr).

- Experiments exclusively in dipole flow fields with 100% recovery of conservative tracers.

- Maximum stock activity of 740 MBq for the radionuclides of Table 3, and maximum injection activity of 7.4 MBq for each radionuclide in each experiment.

- Recovery of radionuclides in two tanks, at the end of the withdrawal-flow line, with subsequent decay of short-lived radionuclides, and further decontamination of long-lived radionuclides (^{22}Na$^+$ and ^{137}Cs$^+$; see Table 3).

^{22}Na$^+$ was pumped to a mobile on-site ion-exchange facility using antimony pentoxide hydrate as the sorbent. This procedure reduced the activity of ^{22}Na$^+$ in the water to < 0.4 Bq l^{-1}. ^{137}Cs$^+$ was pumped to an ion-exchange column filled with a composite absorbent consisting of nickel hexacyanoferrate as the active component, built onto a matrix of polyacrylonitrile (Sebesta et al., 1994). This procedure reduced the activity of ^{137}Cs$^+$ to < 0.2 Bq l^{-1}. Subsequently, the solutions were discharged to the Aare River.

3. Results and discussion

3.1. Overview

The results of the dipole injection–withdrawal experiments are subdivided into two sections, those from the shorter flow field (1.7 m flow distance) and those from the longer one (4.9 m flow distance). The cationic radionuclides used as tracers were weakly sorbing (^{24}Na$^+$ and ^{22}Na$^+$), moderately sorbing (^{85}Sr^{2+} and ^{86}Rb$^+$), and strongly sorbing (^{137}Cs$^+$). The breakthrough curves (BTCs) of these tracers are plotted in Figs. 4–8. A normalization of tracer concentrations (C) to the injected mass or activity, M_0, i.e., C/M_0 [mg ml^{-1} mg^{-1}; Bq ml^{-1} Bq^{-1}], allowed comparison between BTCs of different tracers and different flow fields. An integration of the concentration with time (area under the BTCs) times the flow rate yields curves of tracer recovery as a function of time [$R(t) = (Q(\int_0^\infty C(t)\mathrm{d}t))/M_0$]. Table 4 summarizes the experimental results. The groundwater flow velocities derived from the BTCs of uranine were between 1.3 and 2.0 m h^{-1} in the shorter flow field, and 0.9 m h^{-1} in the longer flow field. The BTCs of the radionuclides were subject to counting statistics as a function of time and total activity of the input solution. The linearity of the γ-counters was tested in that different aliquots were taken from input solutions. At a dilution range between 10^0–10^{-5}, linear regression lines were obtained between expected and measured activities for Na and Sr, indicating linearity between γ-count rate and activity (Eikenberg et al., 1994). An overall error in the concentration measurements was in the order of 5% at high concentrations, and went up to about 30% near background.

The results are shown in Table 5 (shorter flow field) and Table 6 (longer flow field) using three parameters which are derived from the BTCs of uranine and compared with
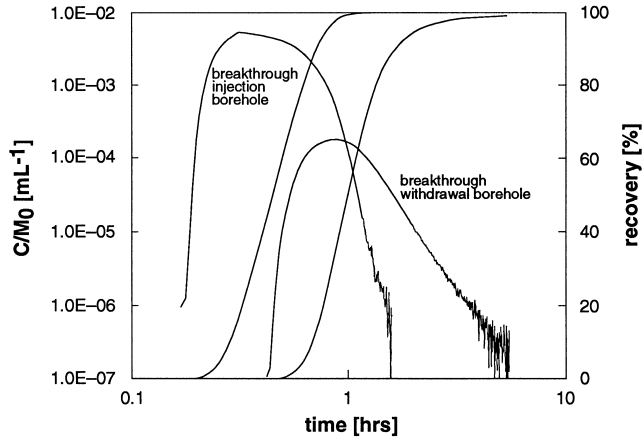
Fig. 5. 'Breakthrough injection bore hole': uranine concentration–time distribution (CTD) and recovery curves in injection bore hole (P_I); 'Breakthrough withdrawal bore hole': uranine BTC and recovery curves in withdrawal bore hole (P_W). Note small delay resulting in influence of BTC in P_W by CTD in P_I; recovery curves shown at linear vertical axis, at right-hand side; shorter flow distance of 1.7 m; Run no. 75.

the BTCs of the sorbing radionuclides: (i) the peak-height reduction [$(C_{peak}/M_0)_{red}$], (ii) the peak retardation (R_{peak}), and (iii) the '50%-retardation' ($R_{50\%}$). The three parameters are drawn directly from the experimental BTCs, as follows: the peak-height reduction is the ratio of the relative uranine peak concentration divided by the relative peak concentration of the respective radionuclide. The peak retardation is the ratio of the peak time of the respective radionuclide divided by the peak time of uranine. It is a measure of the delay of the radionuclide's median residence time compared to that of
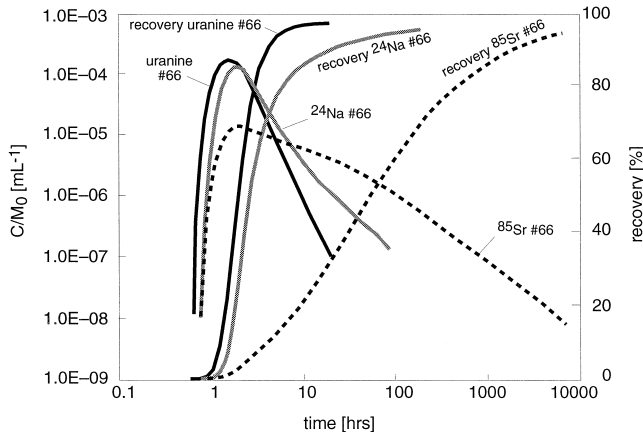

Fig. 6. Tracer concentration–time distribution as breakthrough curve (BTC) of uranine, ^{24}Na$^+$, and ^{85}Sr^{2+} (Run no. 66) in double-logarithmic scale; concentration normalized to injected mass or activity (C/M_0), and corrected for radioactive decay; shorter flow distance of 1.7 m; recovery curves shown at linear vertical axis, at right-hand side.
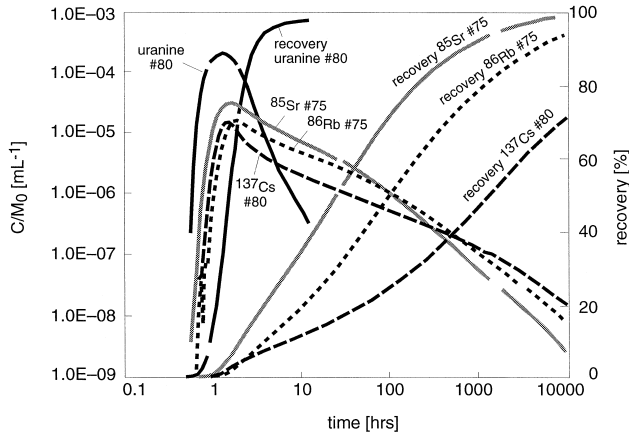
Fig. 7. Tracer concentration–time distribution as breakthrough curve (BTC) of uranine (Run no. 80), $^{85}Sr^{2+}$ and $^{86}Rb^{+}$ (Run no. 75), and $^{137}Cs^{+}$ (Run no. 80), in double-logarithmic scale (Runs no. 75 and 80 combined); concentration normalized to injected mass or activity (C/M_0), and corrected for radioactive decay; shorter flow distance of 1.7 m; recovery curves shown at linear vertical axis, at right-hand side.

uranine. The 50% retardation is the ratio of the time of 50% recovery of the respective radionuclide divided by the time of 50% uranine recovery. It is a measure of the delay of the mean radionuclide residence time with respect to that of uranine. The three parameters form a basis for transport modeling and give a qualitative indication of transport processes of the radionuclides.

The tracer injection function of the larger flow field was such that the uranine concentration in the packed-off section of the injection bore hole was at background
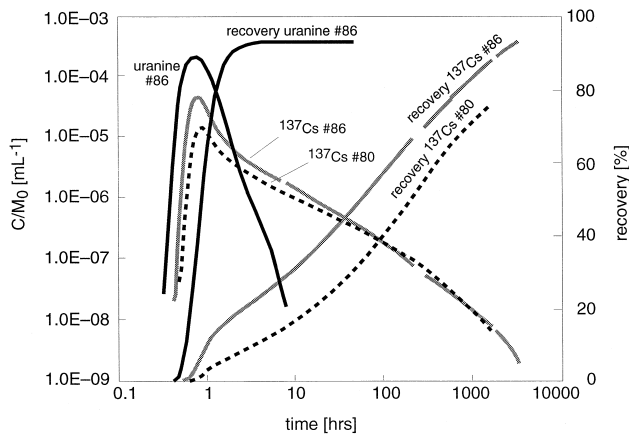

Fig. 8. Tracer concentration–time distribution as breakthrough curve (BTC) of uranine and $^{137}Cs^{+}$, in double-logarithmic scale; concentration normalized to injected mass or activity (C/M_0), and corrected for radioactive decay; shorter flow distance of 1.7 m; recovery curves shown at linear vertical axis, at right-hand side. tracer concentration: 2.7×10^{-5} M (carrier-free; Run no. 80) and about 3×10^{-2} M (with Cs^{+}-carrier, Run no. 86).

Table 4
Results of pulse–stimulus experiments with uranine and sorbing radionuclide tracers

Run number	Flow distance (m)	Tracer	M_0 (mg) or (MBq)	C_{peak}/M_0 (ml^{-1})	$t(C_{peak}/M_0)$ (h)	$t(50\%)$ (h)
50	4.9	Uranine	0.0630	2.4×10^{-5}	3.3	5.5
		Na-22	0.91	7.7×10^{-6}	4.7	17
		Sr-85	5.3	1.0×10^{-7}	178	2000
66	1.7	Uranine	0.00946	1.8×10^{-4}	1.1	1.3
		Na-24	0.40	1.3×10^{-4}	1.1	1.4
		Sr-85	3.1	1.2×10^{-5}	1.1	15
75	1.7	Uranine	0.0117	2.0×10^{-4}	0.82	1.1
		Sr-85	2.7	3.2×10^{-5}	0.90	8.8
		Uranine[a]	0.0884	1.8×10^{-4}	0.87	1.2
		Rb-86[a]	11.7	1.6×10^{-5}	1.0	25.5
80	1.7	Uranine	0.0080	2.1×10^{-4}	0.76	0.86
		Cs-137	6.4	1.2×10^{-5}	0.85	180
86	1.7	Uranine	0.0074	2.2×10^{-4}	0.70	0.85
		Cs-137[b]	6.5	4.6×10^{-5}	0.75	5
90	4.9	Cs-137	6.5	3.9×10^{-9}	2530	$\approx 30\,000$

M_0: injected mass, or activity.
C_{peak}/M_0: relative maximum (peak) mass or activity concentration [mg ml^{-1}/mg^{-1}; MBq ml^{-1}/MBq^{-1}].
$t(C_{peak}/M_0)$: time at which peak concentration occurred.
$t(50\%)$: time of 50% recovery.
[a] Injected one week later.
[b] Carrier added to Cs-137 radioactivity, by factor of 1000.

long before the first arrival of the tracer in the withdrawal bore hole. In the shorter flow field, however, uranine appeared in the withdrawal bore hole at a time, at which the concentration in the injection bore hole was still significant (see Fig. 5). The tracer was less diluted in the smaller flow field than in the larger one. Therefore, modeling the breakthrough and the recovery of the tracers required the knowledge of the complete input function.

Table 5
Shorter flow field, parameter ratios derived from radionuclide and uranine breakthrough curves

Run number	Radionuclide	$(C_{peak}/M_0)_{red}$	R_{peak}	$R_{50\%}$
66	Na-24	1.4	1	1.1
66	Sr-85	15	1	14
75	Sr-85	6.3	1.1	8.0
75	Rb-86	11	1.1	21.3
80	Cs-137	17.5	1.1	209
86	Cs-137	4.8	1.1	68

$(C_{peak}/M_0)_{red}$: radionuclide peak-height reduction, relative maximum (peak) activity concentration of uranine, divided by relative peak concentration of sorbing radionuclide.
R_{peak}: radionuclide peak retardation, time at which peak of sorbing tracer appeared, divided by time at which uranine peak appeared.
$R_{50\%}$: '50%-retardation', i.e., radionuclide retardation at time of 50% recovery.

Table 6
Longer flow field, parameter ratios derived from radionuclide and uranine breakthrough curves

Run number	Radionuclide	$(C_{peak} / M_0)_{red}$	R_{peak}	$R_{50\%}$
50	Na-22	3.1	1.4	3.2
50	Sr-85	240	54	364
90	Cs-137	6154	767	≈ 5450

$C_{peak} / M_0)_{red}$: radionuclide peak-height reduction, relative maximum (peak) activity concentration of uranine, divided by relative peak concentration of sorbing radionuclide.
R_{peak}: radionuclide peak retardation, time at which peak of sorbing tracer appeared, divided by time at which uranine peak appeared.
$R_{50\%}$: '50%-retardation', i.e., radionuclide retardation at time of 50% recovery.

Experiments with the same withdrawal flow rate, but with different injection flow rates allowed an assessment of the optimal flow rate to obtain maximum tracer recovery. The flow field with a value of β of about 15 resulted in a BTC with a single sharp concentration peak (monomodal), subsequent long tailing and full uranine recovery. A flow field with β of about 3, however, resulted in a BTC with two peaks (bimodal) and recovery rates of < 100%. Migration through one of the water-conducting zones might have been so much restricted at β of about 15 that the respective peak was suppressed by the magnitude of the peak resulting from migration through the other zone. Less asymmetrical injection–withdrawal flow fields (small value of β) have somewhat smaller flow velocities, but are still far from being representative for the potential sites of radioactive wastes disposal. The groundwater flow velocities are higher at the hydraulic gradients of a dipole flow system than at natural flow conditions. They are, furthermore, more sensitive to heterogeneities of the transmissivity within the fracture system and thus have a tendency to result in multiple-peak responses to tracer injection (see Moreno and Tsang, 1991; for details, see Frick, 1994).

Effects of interchanging injection and withdrawal bore holes (reverse flow), were investigated with two sets of experiments in the longer flow field. Each experiment of the two sets was conducted at about the same flow rates, one with flow towards the drift, and one with reverse flow, i.e., away from the drift. The reverse flow field was found not to be bounded in that in the order of 30–40% of the tracer were lost.

3.2. Shorter flow field (1.7 m flow distance; Figs. 6–8)

In the shorter flow field, the BTCs and the recovery curve of uranine were compared with those of the sorbing radionuclides, $^{24}Na^+$ and $^{85}Sr^{2+}$ (Run no. 66; Fig. 6), $^{85}Sr^{2+}$ and $^{86}Rb^+$ (Run no. 75; Fig. 7), and $^{137}Cs^+$ (Runs no. 80 and 86; Fig. 8). The groundwater flow velocity increased slightly with each experiment, in spite of identical injection- and withdrawal-flow rates. This can be judged from Table 4, where the times of uranine peak concentration and of 50% recovery decreased from 1.1 (Run no. 66) to 0.7 h (Run no. 86), and from 1.3 (Run no. 66) to 0.85 h (Run no. 86), respectively. In fact, some wash-out of particulate matter was observed in the filters of the tubing from the withdrawal bore hole, which could be the reason for the observed decrease in tracer

residence time. Given that the values for porosity, hydraulic gradient and flow distance in the fracture remained unchanged, a change of the value for hydraulic conductivity of about 50% due to wash-out of fault gouge does not seem unrealistic.

Only insignificant peak retardation was observed for the sorbing tracers (Column 4 of Table 5). From the steeply rising leading edge of the BTCs and the peaks, which were similar for all tracers used, it was concluded that a rapid transport of the tracers through water-conducting zones predominates and that sorption processes played a minor role at the beginning of the experiments. The initial breakthrough occurred after about 1 h. Only a small fraction of the injected uranine tracer mass contributed to the peak breakthrough, and large differences in groundwater flow velocity probably exist between the center of the fracture and the surfaces of the rock. The trailing edge of the BTCs fell considerably less than the rise of the leading edge. The fraction of the injected tracer that was transported with delay is responsible for the long tailing of the trailing edge. This tailing is controlled by sorption, tracer diffusion in and out of the fault, or both (matrix diffusion, see Hadermann and Heer, 1996). Table 5 shows that retardation becomes of importance only at the trailing edge of the BTCs (50%-retardation > 1 for sorbing tracers). Sorption of the radionuclides was assumed to be fully reversible in the shorter flow field, in that the tracers revealed either a full recovery of the injected activity, or the recovery curve could be extrapolated to 100%. Complete elution of these ions during desorption was found in the static batch experiments of Aksoyoglu et al. (1990). These experiments used disaggregated mineral surfaces of mylonitic rock materials from the GTS, which is the same as that of the local experimental site. The contact time of the water with rock surfaces was much longer in the batch laboratory experiments than in the field migration experiments. Thus comparisons between laboratory and field work may be limited.

$^{24}Na^+$. The BTC of Na was similar to that of uranine (Fig. 6) with values of about 1 for the parameters shown in Table 5. A model simulation of Heer and Hadermann (1994) of this BTC used a best-fit distribution coefficient of $K_d = 0.13$ ml g^{-1} for bulk sorption of Na in a porous matrix, which was based on various laboratory sorption experiments (batch and dynamic infiltration) of Aksoyoglu et al. (1990), Baeyens and Bradbury (1989) and Smith (1992), and on a field hydrogeochemical experiment (Eikenberg et al., 1991).

$^{85}Sr^{2+}$, $^{86}Rb^+$. The general shape of the BTCs of both radionuclides, Sr and Rb (see Fig. 7) was similar. Table 5 shows that the values for peak-height reduction and 50%-retardation of Sr and Rb were significantly above one. Sorption of Rb was somewhat stronger than that of Sr. A model simulation by Heer and Hadermann (1994) of the BTC of Sr with bulk sorption in the porous matrix used a best-fit distribution coefficient of $K_d = 21$ ml g^{-1}, which was based on the same experiments as above for Na. The trailing edges of the BTCs decreased with time as $t^{-3/2}$, at times later than about 10 h. This was interpreted by Heer and Hadermann (1994) to be a strong support for their model of matrix diffusion. At the end of Experiment no. 75 (1369 h = 57 days, about 3 half lives of ^{86}Rb), nearly 90% of the injected Rb has decayed and activities returned to background levels.

$^{137}Cs^+$. In Experiment no. 80, carrier-free ^{137}Cs$^+$ was injected to keep the concentration of the injected radiocesium as low as possible, and to rule out changes of the

sorption isotherm. The maximum concentration of total Cs in the injection bore hole of about 10^{-7} M during the experiment was about 100 times higher than the natural background (Table 2). The general shape of the BTC of Cs in the withdrawal bore hole was similar to that of Rb and Sr in Fig. 6. However, the 50%-retardation was significantly higher. Within this period, the recovery of Cs amounted to 76%. From the results of Experiment no. 80, it was assumed that the BTC of Cs is dominated by the same processes as were the BTCs of Sr and Rb. Cremers et al. (1988) showed that the Cs sorption process is governed by isotope exchange, at low radiocesium concentrations, and by a preferential sorption on frayed edge sites of micas and clays, at higher concentrations.

To observe the effect of a high total Cs concentration in the groundwater on the transport behavior of radiocesium in the field, a carrier of inactive Cs^+ of a factor of about 1000 was added to the radionuclide in Experiment no. 86. This experiment was held under flow conditions similar to those of Experiment no. 80. The carrier-containing tracer sorbed less extensively than the carrier-free one. The peak retardation relative to uranine was about the same in both experiments. The following results of this experiment were interpreted as effects of non-linear sorption (Fig. 8): the peak-height reduction was lower in Experiment no. 86 than in no. 80 by a factor of 3.6. The 50%-retardation was lower with carrier Cs by a factor of 3.1. After about 900 h (somewhat more than 1 month), the recovery rate of $^{137}Cs^+$ amounted to 93% in Experiment no. 86, which is 17% more than that of no. 80 after 2 months. Aksoyoglu (1990) and Aksoyoglu et al. (1990) investigated the sorption behavior of Cs, again on disaggregated mineral surfaces of mylonitic rock materials from the GTS site. They found distribution coefficients of Cs which showed a non-linear sorption isotherm and which were dependent on the potassium concentrations in the groundwater.

3.3. Longer flow field (4.9 m flow distance; Fig. 9)

As was the case in the shorter flow field, a full recovery of uranine in all the experiments indicated that the flow domain was bounded. The groundwater flow velocity, calculated from the 50%-recovery of uranine, was smaller in the longer flow field (about 1 m h^{-1}; shorter flow field: about 1.9 m h^{-1}; see Table 4). The peak concentration in the longer flow field was smaller by more than two orders of magnitude. In the longer flow field, the BTCs and recovery curves of uranine were compared with those of the sorbing radionuclides, $^{22}Na^+$ and $^{85}Sr^{2+}$ (Run no. 50) and $^{137}Cs^+$ (Run no. 90). A comparison of the shorter with the longer flow field resulted in the following differences:

(a) Shorter flow field;
- no peak retardation observed for any radionuclide tracer;
- leading edge of tracer BTC dominated by rapid advection–dispersion through highly transmissive zones;
- small peak-height reduction;
- 50%-retardation indicated retardation with mainly matrix diffusion and some sorption and desorption, only at trailing edge of BTC.
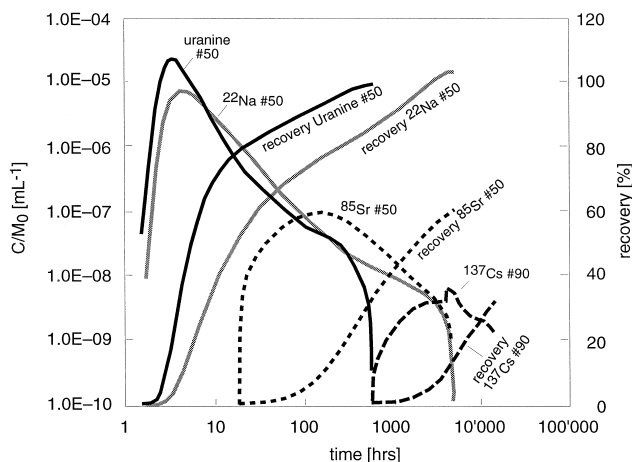
Fig. 9. Tracer concentration–time distribution as breakthrough curve (BTC) of uranine, ^{22}Na$^+$, ^{85}Sr^{2+} (Run no. 50) and ^{137}Cs$^+$ (Run no. 90), in double-logarithmic scale (Runs no. 50 and 90 combined); concentration normalized to injected mass or activity (C/M_0), and corrected for radioactive decay; larger flow distance of 4.9 m; recovery curves shown at linear vertical axis, at right-hand side. Apparent second peak in Cs BTC, due to malfunction of pumps maintaining dipole flow field.

(b) Longer flow field;
 · significant peak retardation and peak-height reduction for the reactive radionuclide tracers;
 · the 50%-retardation of the reactive tracers indicated that the retardation of the radionuclides represents sorption and matrix diffusion, which dominate radionuclide transport.

^{22}Na$^+$. With respect to that of uranine in the same experiment, the BTC of Na revealed a slight peak-height reduction, peak retardation and 50%-retardation. The values for the parameters 'peak-height reduction' and '50%-retardation' of Na were higher in the longer flow field, by a factor of 2–3. As in the shorter flow field, the full recovery of Na showed that sorption was reversible. Hadermann and Heer (1996) fitted the BTC of uranine and Na (K_d for Na: 0.13 ml g^{-1}) with good agreement and found strong support for their transport model which includes matrix diffusion. The Na peak was dominated by rapid advection–dispersion transport through highly transmissive channels as was the case in the shorter flow field, but was less pronounced than that of uranine. At times much larger than the occurrence of the peak (> 10 h), the trailing edges of the uranine and the ^{22}Na$^+$ BTCs decreased with time at $t^{-3/2}$, as was shown for radionuclides in the shorter flow field.

^{85}Sr. The general shape of the BTC of Sr in Fig. 9 differed considerably from that of Na (high values for peak-height reduction, peak retardation and 50%-retardation, see Table 6). Compared with the short flow field, the peak-height reduction and 50%-retardation of Sr were accentuated by a factor of 16 and 29, respectively. At larger transport distances, sorption and matrix diffusion are the major transport processes, while advection–dispersion in highly transmissive zones is of less importance. At the

end of Experiment no. 50 (196 days, about 3.5 half lives of $^{85}Sr^{2+}$), when 92% of the radionuclide had decayed, only about 60% of Sr were recovered. From an extrapolation of the BTC and assuming fully reversible condition, a complete recovery could be expected to occur after about 50 years. Hadermann and Heer (1996) fitted the BTC of Sr with their model (K_d for Sr: 21 ml g^{-1}) and found that bulk sorption combined with matrix diffusion in the porous matrix dominate the transport through the longer flow field. Sorption could also take place on fracture surfaces away from the immediately accessible flow field.

$^{137}Cs^+$. An experiment with $^{137}Cs^+$ in the longer flow field was planned to complete the data set of experiments with weakly- to strongly-sorbing radionuclides of alkaline and alkaline-earth metals. The aim of this experiment was to show the influence of the longer flow distance on radionuclide transport, and to test a model prediction, which was based on the results of laboratory studies and previous field experiments in the shorter flow field. Given the peak-height reduction of $^{85}Sr^{2+}$ of 240 in Experiment no. 50 (Table 6) and the maximum permitted injection activity for $^{137}Cs^+$ of 7.4 MBq, it was not clear whether a breakthrough of $^{137}Cs^+$ could be detected at all in the longer flow field. The preliminary predictions of relative peak $^{137}Cs^+$ concentrations and the time at which the peak could occur (Heer, personal communication, 1994) ranged from 7–70 Bq l^{-1}, and between 30 days and about 1 year, respectively. The large range of values resulted from the high variability of laboratory values for K_d of Cs$^+$ of between 134 and 1420 ml g^{-1} used for the predictions (Aksoyoglu et al., 1990). The detection limit of ^{137}Cs was found in the laboratory to be in the order of 1 Bq l^{-1}; thus a BTC could be expected to be observed within 1–2 orders of magnitude. From this it was decided to start the experiment on July 18, 1994, which was a challenge for the efficiency of the equipment set-up, e.g., pump discharge rates, for the stability of the flow field over possibly many years.

A relative peak concentration of $C_{peak}/M_0 = 3.9 \times 10^{-9}$ ml^{-1} (22 Bq l^{-1}), which occurred after about 4 months, showed that the peak-height reduction and the peak retardation were higher for Cs than for Sr (Table 6). Based on a model fit of the BTC, the time of the 50%-retardation was expected to be reached at about 3 years after injection, later than that of Sr by a factor of 15. A comparison with the results of the Cs experiment in the shorter flow field (Run no. 80) revealed that the peak retardation was higher by a factor of about 700. The longer residence time in the shear zone allowed the diffusion and the sorption in the matrix to be dominant over advective–dispersive transport in the highly transmissive channels. The peak-height reduction and the 50%-retardation were higher in the longer flow field by a factor of about 1300 and about 80, respectively. It is not known, whether sorption takes place on fracture surfaces somewhat away from the main flow path, or on the porous matrix, as was suggested by Heer and Hadermann (1994).

3.4. Selectivity sequence

Many variations of an affinity or selectivity sequence have been proposed, in which equivalent amounts of cations are arranged according to their relative affinity for an

exchange site, especially for clays assuming fixed-charged surfaces (e.g., Sposito, 1989). Such a sequence can usually not be applied rigorously because of heterogeneous geochemical conditions. Here a selectivity sequence was established with the values of the time of 50% recovery of the sorbing tracers. To obtain a value for Ca, for which no radionuclide suitable for tracer experiments was available, the results were compared with those from the hydrogeochemical equilibrium experiment of Eikenberg et al. (1991). Their experiment consisted in a continuous miscible displacement of the groundwater in the flow field (step stimulus) by a groundwater of a slightly different ionic composition. These authors determined the time required for the main cationic compounds to reach a new steady-state concentration and defined a retardation factor as the time at which 50% of the cation concentration change occurred, divided by the time at which 50% of the Cl^- concentration change occurred (Cl^- assumed to be the conservative tracer). They found values for their retardation factor of about 3 for Na^+ and Ca^{2+}, of about 5 for Sr^{2+}, and of more than 6 for Mg^{2+} and K^+. The absolute values cannot be compared in the two experiments with tracers at much lower concentrations. The relative positions in the selectivity sequence of the various compounds are, however, taken to be comparable. The final sequence from the field experiments at the GTS is thus $Na^+ (< Ca^{2+}) < Sr^{2+} < Rb^+ < Cs^+$. It confirms the results of Aksoyoglu et al. (1990), established in the laboratory for the disaggregated mineral surfaces of mylonitic material from the GTS site. An extrapolation from laboratory to field conditions can thus be used for model predictions of radionuclide migration in the particular system studied in the GTS.

4. Conclusions

Two-bore hole injection–withdrawal field migration experiments produced breakthrough curves (BTCs) and recovery curves of the conservative tracer uranine and the sorbing radionuclide tracers $^{22}Na^+$, $^{24}Na^+$, $^{85}Sr^{2+}$, $^{86}Rb^+$ and $^{137}Cs^+$ in a single shear zone in granodiorite at the Grimsel Test Site. The tracer experiments in two different flow fields in the granodioritic rock (linear distance: 1.7 and 4.9 m) resulted in breakthrough curves which lasted between 10 h and 1.6 years and contained concentration monitoring over about eight orders of magnitude. The acquisition of high-quality data required a significant investment of time, energy, and money. Compared to the dynamic and static laboratory experiments, the observation of radionuclide transport in a natural shear zone under chemically almost undisturbed conditions allowed the identification of processes at a larger temporal and spatial scale. Transport models could be tested by comparing field observations with model predictions, and subsequent adjustment of the predictions. The sequence of the affinity of the alkaline and alkaline-earth cationic radionuclides for exchange sites did not exhibit a scale effect from the laboratory to the field, which adds confidence to models used for predictions of BTCs in field experiments in similar environments. The chosen experimental temporal and spatial scale is, however, different from that in a radioactive wastes repository. There, the groundwater flow velocities are much smaller, and, therefore, the time for diffusive and sorptive processes to take place is much greater.

Field experiments have been expanded to other safety-relevant redox-sensitive radionuclides of, e.g., Se, Co, U, Np, Eu and Tc. As the final stage of the Migration Program at the Grimsel Test Site, part of the shear zone between the injection and the withdrawal bore hole has been excavated, allowing a direct description of the pathway of radionuclides in the fracture by mapping the radionuclide distribution in the pore space. This will help improving the prediction capacity of the models by producing a better conceptual model of transport in the experimental shear zone. The overall Migration Program will yield an improved understanding of the processes governing radionuclide transport infractured rock and has required in-depth cooperation among modelers, laboratory and field experimentalists.

Acknowledgements

References

Abelin, H., Birgersson, L., Gidlund, J., Neretnieks, I., 1991. A large-scale flow and tracer experiment in granite: 1. Experimental design and flow distribution. Water Resour. Res. 27 (12), 3107–3117.

Aksoyoglu, E.S., 1990. Cesium sorption on mylonite. J. Radioanal. Nucl. Chem. 140, 301–313.

Aksoyoglu, E.S., Bajo, C., Mantovani, M., 1990. Grimsel test site: batch sorption experiments with iodine, bromine, strontium, sodium and cesium on Grimsel mylonite. NAGRA Tech. Report NTB 91-06 and PSI Report 83, NAGRA, Wettingen, Switzerland.

Baeyens, B., Bradbury, M.H., 1989. Selectivity coefficients and estimates of in situ sorption values for mylonite. In: Bradbury, M.H. (Ed.), Laboratory Investigations in Support of the Migration Experiments at the Grimsel Test Site. NAGRA Tech. Report NTB 88-23 and PSI Report 28, Wettingen, Switzerland.

Bajo, C., Hoehn, E., Keil, R., Baeyens, B., 1989. Chemical characterisation of the groundwater from fault zone AU 96 m. In: Bradbury, M.H. (Ed.), Laboratory Investigations in Support of the Migration Experiments at the Grimsel Test Site. NAGRA Tech. Report NTB 88-23 and PSI Report 28, NAGRA, Wettingen, Switzerland.

Behrens, H., 1983. Comparison of radioactive and non-radioactive tracers. Tracer Methods in Isotope Hydrology. Proc. Adv. Group Meet. IAEA, Vienna, September 27–October 1, 1982, pp. 173–186.

Bossart, P., Mazurek, M., 1991. Grimsel test site: structural geology and water flow-paths in the migration shear-zone. NAGRA Tech. Report NTB 91-12, NAGRA, Wettingen, Switzerland.

Bradbury, M., Baeyens, B., 1992. Modeling the sorption of Cs: application to the Grimsel migration experiment. PSI Annu. Rep., Annex IV, PSI Nucl. Energy Res., Progr. Rep. 1992. Paul Scherrer Inst., Villigen, Switzerland, pp. 59–64.

Cremers, A., Elsen, A., de Preter, P., Maes, A., 1988. Quantitative analysis of radiocesium retention in soils. Nature 335, 247–249.

Eikenberg, J., Baeyens, B., Bradbury, M.H., 1991. The Grimsel Migration Experiment: a hydrogeochemical equilibration test. NAGRA Tech. Report NTB 90-39 and PSI Report 100, NAGRA, Wettingen, Switzerland.

Eikenberg, J., Frick, U., Fierz, T., Bühler, C., 1992. On-line detection of stable helium isotopes in migration experiments. In: Hötzl, H.H., Werner, A. (Eds.), Tracer Hydrology. Karlsruhe, Balkema, Rotterdam/Brookfield, pp. 77–84.

Eikenberg, J., Hoehn, E., Fierz, T., Frick, U., 1994. Grimsel test site: preparation and performance of migration experiments with radioisotopes of sodium, strontium, and iodine. NAGRA Tech. Report NTB 94-17 and PSI Report 94-11, NAGRA, Wettingen, Switzerland.

Frick, U., 1994, The Grimsel radionuclide migration experiment—a contribution to raising confidence in the validity of solute transport models used in performance assessment. OECD Docum., Nuclear Fuel Agency, Safety Assessment of Radionuclide Waste Repositories, GEOVAL '94—Validation thorough model testing. Proc. of an NEA/SKI Symp., Paris, France, October 11–14, 1994, pp. 245–272.

Frick, U., Alexander, W.R., Baeyens, B., Bossart, P., Bradbury, M.H., Bühler, Ch., Eikenberg, J., Fierz, T., Heer, W., Hoehn, E., McKinley, I.G., Smith, P.A., 1992. Grimsel test site. The radionuclide migration experiment—overview of investigations 1985–1990. NAGRA Tech. Report NTB 91-04 and PSI Report 120, NAGRA, Wettingen, Switzerland.

Hadermann, J., Heer, W., 1996. The Grimsel (Switzerland) migration experiment: integrating field experiments, laboratory investigations and modelling. J. Contam. Hydrol. 21, 87–100.

Hadermann, J., von Gunten, H.R., McCombie, Ch., McKinley, I.G., 1988. Radionuclide migration in the geosphere—Swiss research activities in laboratory and field experiments and in model validation. Radioactive Waste Manage. Nucl. Fuel Cycle 10 (1–3), 233–255.

Heer, W., Hadermann, J., 1994. Grimsel test site. Modelling radionuclide migration field experiments. NAGRA Tech. Report NTB 94-18 and PSI-Report 94-13, NAGRA, Wettingen, Switzerland.

Hoehn, E., Fierz, T., Thorne, P., 1990. Hydrogeological characterisation of the migration experimental area at the Grimsel test site. NAGRA Tech. Report NTB 89-15 and PSI Report 60, NAGRA, Wettingen, Switzerland.

HSK (1993). Guideline HSK-R-21/e, Protection Objectives for the Disposal of Radioactive Wastes. Swiss Federal Nuclear Safety Inspectorate (HSK) and Federal Commission for the Safety of Nuclear Installations (KSA), revised version. CH-5232 Villigen-HSK, Switzerland, November 1993.

Klockars, C.E., Persson, O., Tullborg, E.-L., Larson, S.A., Andersson, K., Allard, B., Torstenfelt, B., 1983. Migration experiments in Studsvik. SKBF/KBS Tech. Report 83-18, Svensk Kärnbränsleförsörjning, Stockholm, Sweden.

McKinley, I.G., Alexander, W.R., Bajo, C., Frick, U., Hadermann, J., Herzog, F., Hoehn, E., 1988. The radionuclide Migration Experiment at the Grimsel Rock Laboratory, Switzerland. Sci. Basis Nucl. Waste Manage. XI, 179–187.

Meyer, P., Mazurek, M., Alexander, W.R., 1989. Petrographic and mineralogic characterization of fault zones AU96m and AU126m. In: Bradbury, M.H. (Ed.), Laboratory investigations in support of the migration experiments at the Grimsel Test Site. NAGRA NTB 88-23 and PSI Report 28, NAGRA, Wettingen, Switzerland.

Moreno, L., Tsang, Ch.-F., 1991. Multiple-peak response to tracer injection tests in single fractures: a numerical study. Water Resour. Res. 27 (8), 2143–2150.

NAGRA, 1994. Kristallin-I, Safety Assessment Report. NAGRA NTB 93-22E, NAGRA, Wettingen, Switzerland, 430 pp.

Neretnieks, I., Eriksen, T., Tähtinen, P., 1982. Tracer movement in a single fissure in granitic rock: some experimental results and their interpretation. Water Resour. Res. 18 (4), 849–858.

Nowakowski, K.S., Evans, G.V., Lever, D.A., Raven, K.G., 1985. A field experiment of measuring hydrodynamic dispersion in a single fracture. Water Resour. Res. 21 (8), 1165–1174.

Sebesta, F., Motl, A., John, J., Prazsy, M., Binka, J., 1994. Composite ion-exchangers and their possible use in treatment of low/intermediate level liquid radioactive wastes. In: Proc. 1993 Int. Conf. Nucl. Wastes Management and Environmental Remediation, Sept. 5–11, 1993, Prague. ASME, New York, 3, 871–873.

Smart, P.L., Laidlaw, I.M.S., 1977. An evaluation of some fluorescent dyes for water tracing. Water Resour. Res. 13 (1), 15–33.

Smith, P., 1992. Modelling of laboratory high-pressure infiltration experiments. NAGRA NTB 91-33, and PSI Report 116, NAGRA, Wettingen, Switzerland.

Sposito, G., 1989. The Chemistry of soils. Oxford Univ. Press, New York, 277 pp.